

Cross-section measurement for quasi-elastic production of charmed baryons in νN interactions

The CHORUS Collaboration

Abstract

A study of quasi-elastic production of charmed baryons in charged-current interactions of neutrinos with the nuclear emulsion target of CHORUS is presented. In a sample of about 46,000 interactions located in the emulsion, candidates for decays of short-lived particles were identified by using new automatic scanning systems and later confirmed through visual inspection. Criteria based both on the topological and kinematical characteristics of quasi-elastic charm production allowed a clear separation between events of this type and those in which charm is produced in deep inelastic processes. A final sample containing 13 candidates consistent with quasi-elastic production of a charmed baryon with an estimated background of 1.7 events was obtained. At the average neutrino energy of 27 GeV the cross-section for the total quasi-elastic production of charmed baryons relative to the νN charged-current cross-section was measured to be $\sigma(QE)/\sigma(CC) = (0.23_{-0.06}^{+0.12}(stat)_{-0.03}^{+0.02}(syst)) \times 10^{-2}$. Through an analysis of the topology at the production and decay vertices the relative cross-sections were measured separately for singly (Λ_c^+ , Σ_c^+ , Σ_c^{+*}) and doubly (Σ_c^{++} , Σ_c^{++*}) charged baryons.

To be published in Phys. Lett. B

The CHORUS Collaboration

A. Kayis-Topaksu, G. Onengüt
Çukurova University, Adana, Turkey

R. van Dantzig, M. de Jong, O. Melzer, R.G.C. Oldeman¹, E. Pesen, F.R. Spada², J.L. Visschers
NIKHEF, Amsterdam, The Netherlands

M. Güler³, U. Köse, M. Serin-Zeyrek, R. Sever, P. Tolun, M.T. Zeyrek
METU, Ankara, Turkey

M.G. Catanesi, M. De Serio, M. Ieva, M.T. Muciaccia, E. Radicioni, S. Simone
Università di Bari and INFN, Bari, Italy

A. Bülte, K. Winter
Humboldt Universität, Berlin, Germany⁴

B. Van de Vyver^{5,6}, P. Vilain⁷, G. Wilquet⁷
Inter-University Institute for High Energies (ULB-VUB) Brussels, Belgium

G. L. Pittoni, B. Saitta
Università di Cagliari and INFN, Cagliari, Italy

E. Di Capua
Università di Ferrara and INFN, Ferrara, Italy

S. Ogawa, H. Shibuya
Toho University, Funabashi, Japan

A. Artamonov⁸, M. Chizhov⁹, M. Doucet¹⁰, I.R. Hristova⁹, T. Kawamura, D. Kolev⁹, H. Meinhard,
J. Panman, I.M. Papadopoulos, S. Ricciardi¹¹, A. Rozanov¹², R. Tsenov⁹, J.W.E. Uiterwijk, P. Zucchelli¹³
CERN, Geneva, Switzerland

J. Goldberg
Technion, Haifa, Israel

M. Chikawa
Kinki University, Higashiosaka, Japan

E. Arik
Bogazici University, Istanbul, Turkey

J.S. Song, C.S. Yoon
Gyeongsang National University, Jinju, Korea

K. Kodama, N. Ushida
Aichi University of Education, Kariya, Japan

S. Aoki, T. Hara
Kobe University, Kobe, Japan

T. Delbar, D. Favart, G. Grégoire, S. Kalinin, I. Maklioueva
Université Catholique de Louvain, Louvain-la-Neuve, Belgium

P. Gorbunov⁶, V. Khovansky, V. Shamanov, I. Tsukerman
Institute for Theoretical and Experimental Physics, Moscow, Russian Federation

N. Bruski, D. Frekers
Westfälische Wilhelms-Universität, Münster, Germany³

K. Hoshino, J. Kawada, M. Komatsu, M. Miyanishi, M. Nakamura, T. Nakano, K. Narita, K. Niu, K. Niwa,
N. Nonaka, O. Sato, T. Toshito
Nagoya University, Nagoya, Japan

S. Buontempo, A.G. Cocco, N. D'Ambrosio, G. De Lellis, G. De Rosa, F. Di Capua, A. Ereditato, G. Fiorillo,
A. Marotta, M. Messina, P. Migliozi, C. Pistillo, L. Scotto Lavina, P. Strolin, V. Tioukov
Università Federico II and INFN, Naples, Italy

K. Nakamura, T. Okusawa
Osaka City University, Osaka, Japan

U. Dore, P.F. Loverre, L. Ludovici, P. Righini, G. Rosa, R. Santacesaria, A. Satta
Università La Sapienza and INFN, Rome, Italy

E. Barbuto, C. Bozza, G. Grella, G. Romano, C. Sirignano, S. Sorrentino
Università di Salerno and INFN, Salerno, Italy

Y. Sato, I. Tezuka
Utsunomiya University, Utsunomiya, Japan

¹ Now at University of Pennsylvania, Philadelphia, USA.

² And INFN, Roma, Italy

³ Now at Nagoya University, Nagoya, Japan.

⁴ Supported by the German Bundesministerium für Bildung und Forschung under contract numbers 05 6BU11P and 05 7MS12P.

⁵Fonds voor Wetenschappelijk Onderzoek, Belgium.

⁶Now at CERN, 1211 Geneva 23, Switzerland.

⁷Fonds National de la Recherche Scientifique, Belgium.

⁸On leave of absence from ITEP, Moscow.

⁹On leave of absence from St. Kliment Ohridski University of Sofia, Bulgaria.

¹⁰Now at University of Maryland, MD, USA

¹¹Now at Royal Holloway College, University of London, Egham, UK.

¹²Now at CPPM CNRS-IN2P3, Marseille, France.

¹³On leave of absence from INFN, Ferrara, Italy.

1 Introduction

Even though the first experimental data on neutrino-induced charmed-baryon production were obtained in the 1970s in bubble chamber experiments [1], they are still rather scarce when compared with those on charmed mesons.

The study of quasi-elastic (QE) processes such as

$$\nu_\mu n \rightarrow \mu^- \Lambda_c^+ \quad (1)$$

$$\nu_\mu n \rightarrow \mu^- \Sigma_c^+ (\Sigma_c^{+*}) \quad (2)$$

$$\nu_\mu p \rightarrow \mu^- \Sigma_c^{++} (\Sigma_c^{++*}) \quad (3)$$

can provide useful information on the form factors for weak transitions of nucleons into charmed baryons, as well as on the structure of baryons containing a heavy quark [2]–[8]. Also the determination of the cross-section for the above processes constitutes an important step towards their understanding, since the predictions of existing models disagree among themselves by one order of magnitude ([2]–[8]). Furthermore, it was previously pointed out [9] that quasi-elastic charm production might be a way to isolate a pure sample of Λ_c^+ that could be suitable to measure more accurately the absolute branching fractions of that particle.

In a previous paper [10] we presented a measurement of the cross-section for production of Λ_c^+ in νN charged current (CC) interactions. In this paper we focus on the quasi-elastic production of charmed baryons.

Charmed hadrons produced through quasi-elastic processes can be isolated either by selecting events with a small number of charged particles at the interaction vertex with the additional kinematical constraint that the invariant mass of the hadronic system be consistent with that of a charmed baryon, or by searching for one of the peculiar topologies shown in Fig. 1 and corresponding to the three different processes (1)–(3) above.

The first approach has been exploited by bubble chamber experiments which combine high efficiency in measuring charged tracks and long-lived neutral particles (Λ , K_s^0), and good momentum resolution [11]–[16]. The cross-section is then extracted by using Λ_c^+ branching ratios, which however are known with large uncertainties [17].

The second approach requires apparatus with excellent spatial resolution in order to detect the short-lived charmed particle prior to its decay and to reconstruct the multiplicity at the primary vertex. Nuclear emulsions have such a resolution and therefore this approach is suitable for use in *hybrid* experiments, i.e. experiments where a nuclear emulsion target is combined with electronic detectors. E531 [18] – where three events consistent with the process $\nu_\mu n \rightarrow \mu^- \Lambda_c^+ (\pi^0)$ have already been observed – and CHORUS are examples of such experiments. Recently, the development within CHORUS of automatic microscopes that scan nuclear emulsions at unprecedented high speed has allowed the study of charm production in neutrino interactions with a statistics significantly larger than previous similar experiments.

In this paper the results of a search for quasi-elastic charm production from a partial sample of the CHORUS data are reported. In particular, measurements of the cross-sections, relative to CC interactions, of both the inclusive $\nu_\mu N \rightarrow \mu^- C$ and the exclusive $\nu_\mu N \rightarrow \mu^- C^+$, $\nu_\mu N \rightarrow \mu^- C^{++}$ quasi-elastic reactions are presented. C indicates here generically a charmed baryon, while C^+ and C^{++} indicate a charmed baryon of single (Λ_c^+ , Σ_c^+ , Σ_c^{+*}) and double (Σ_c^{++} , Σ_c^{++*}) charge, respectively.

2 Experimental apparatus

CHORUS was designed to search for $\nu_\mu \rightarrow \nu_\tau$ oscillations in the SPS wide-band neutrino beam at CERN through the direct observation of decays of the τ lepton in nuclear emulsions. Since charmed particles have a flight

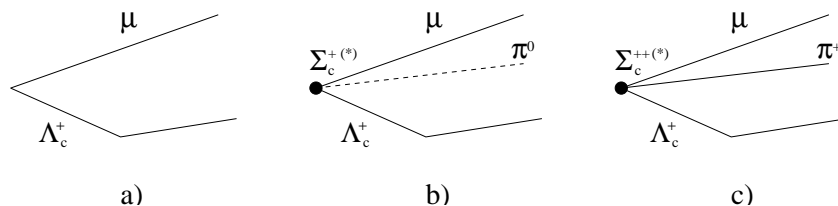


Figure 1: Topology of quasi-elastic production of charmed baryons by neutrinos: a) $\nu_\mu n \rightarrow \mu^- \Lambda_c^+$, b) $\nu_\mu n \rightarrow \mu^- \Sigma_c^+ (\Sigma_c^{+*})$ and c) $\nu_\mu p \rightarrow \mu^- \Sigma_c^{++} (\Sigma_c^{++*})$.

length comparable to that of the τ lepton, the experiment is also suitable to study charm production. The West Area Neutrino Facility (WANF) of the CERN SPS provides an intense beam of neutrinos with an average energy of 27 GeV. It consists mainly of ν_μ with a contamination of 6% $\bar{\nu}_\mu$ and $\sim 1\%$ ν_e . The CHORUS detector was exposed to the neutrino beam during the years 1994–1997, with an integrated flux of 5.06×10^{19} protons on target; in this four-year exposure more than 10^6 neutrino interactions were accumulated in the emulsion target.

The experimental setup is described in Ref. [19]. Here it suffices to mention that it follows a hybrid design that combines a 770 kg nuclear emulsion target with various electronic detectors. The emulsion target was segmented into four stacks, each divided into eight modules. The basic element of a module is a *plate*, two 350 μm layers of emulsion on either side of a 90 μm plastic base of size $36 \times 72 \text{ cm}^2$; 36 plates form a module. Each stack is followed by three interface emulsion sheets with a 90 μm emulsion layer on both sides of a 800 μm thick plastic base – which yields an angular resolution of the order of 1 mrad – and by a set of scintillating fibre trackers which provide an accurate ($\sim 150 \mu\text{m}$ in position and 2 mrad in angle) prediction of particle trajectories into the emulsion stack for the location of the neutrino interaction vertex. The event search in emulsion relies in fact on predictions based upon tracks reconstructed in electronic detectors. These also serve to measure the event kinematics.

For ν_μ CC interactions the muon, identified in the muon spectrometer and reconstructed by the scintillating fibre system, was searched for in the interface emulsion. If found, it was followed upstream by means of an automatic scanning system [20] until no longer found in the target emulsion, thus indicating the existence of a possible vertex. The emulsion plate in which the muon track disappeared is called the *vertex plate*. In total about 150,000 ν_μ CC events have been located in emulsion so far as a result of this procedure.

An automatic scanning system, called ‘Ultra Track Selector’ (UTS) [21], is used to record, within a volume of $1.5 \text{ mm} \times 1.5 \text{ mm}$ for eight consecutive plates (6.3 mm) around the position where the μ^- track disappeared, the spatial coordinates of points along the trajectories of all charged particles that have an angle of less than 400 mrad with respect to the incident neutrino direction. Track segments are searched for only in the most upstream 100 μm of each plate with an efficiency greater than 98%. In what follows, this procedure will be referred to as ‘NetScan’ [22]. The reconstruction of charged-particle trajectories in the NetScan volume allows a general search for the decays of short-lived particles to be performed.

The original analysis was optimized to detect muonic decays of the τ lepton and therefore it excluded events in which the muon had a momentum larger than 30 GeV/c. This selection is no longer applied. The analysis of events with p_μ greater than 30 GeV/c is in progress. The search presented in this paper is limited to events where the measured momentum of the muon is below 30 GeV and is based on a sample of 46,105 ν_μ CC interactions analysed with the NetScan method.

3 Selection of decay topologies

A selection aimed at the construction of a sample to be visually inspected and enriched in Λ_c^+ decays showing the peculiar quasi-elastic topology of Fig. 1 has been developed. The first steps of the selection were applied to *emulsion tracks*¹⁾ and to quantities measured by the electronic detectors; they contained the following requirements:

- one track reconstructed in emulsion must be matched with the muon seen in the electronic detectors, thus defining the location of the neutrino interaction vertex (*vertex plate*);
- another track reconstructed in emulsion must exist whose distance of closest approach to the muon is between 5 and 30 μm , thus signalling the presence of a possible decay vertex;
- this track has to originate in the same plate as the primary vertex (in-plate decay search);
- the event must have at most two tracks at the primary vertex. This is justified since we are looking for low multiplicity topologies (Fig. 1) and at this stage the Λ_c^+ track is too short to be directly detected with the NetScan procedure and will only be seen by the subsequent visual inspection;
- the energy measured in the calorimeter must be less than 10 GeV.

These criteria were applied to a sample of 46,105 ν_μ CC interactions. Of these, 769 events were selected for visual inspection, during which the following set of criteria were applied to obtain the final event sample:

- the presence of a decay is confirmed if the number of charged tracks at the decay vertex is consistent with charge conservation and no other activity (nuclear or Auger electron) is observed;
- decays into a single charged particle are accepted only if the angle between the parent and the decay product (*kink angle*) is greater than 50 mrad;
- flight lengths, measured as the distance between the primary and decay vertices, are required to be greater than 20 μm ; this avoids the loss of efficiency in the visual inspection of decays occurring very close to the primary vertex;
- flight lengths below 200 μm are required to enrich the sample in Λ_c^+ ;

¹⁾ In this search we define an emulsion track as a track reconstructed in the NetScan volume and composed of at least two segments

Decay type	Charged charm	$N_S = 2$	$N_S = 3$
$C1$	33	13	8
$C3$	38	14	13
$C5$	1	1	0
Total	72	28	21

Table 1: Results of the visual inspection for charged charm decays.

- the event is selected as a candidate if, at the primary vertex, it has a charged multiplicity consistent with quasi-elastic charm production ²⁾ ;
- neutrino interactions occurring in the plastic base between emulsion layers are rejected to be able to apply the previous selection on charged multiplicity.

The majority of the inspected events do not exhibit a decay topology, consisting mostly of low-momentum tracks that appear to have a large impact parameter owing to multiple Coulomb scattering and of tracks traversing the emulsion plate [10]. The results of the visual inspection for candidates accepted as a decay of a charged particle are summarized in Table 1. A total of 72 decays were confirmed and in the table they are divided according to the charged multiplicity (1, 3, 5, represented by the digit in the first column) observed in their decay. Of these, 49 satisfy the multiplicity criteria at the neutrino interaction vertex and therefore are considered further as candidates for quasi-elastic production. Details are given in the second and third columns of the table. N_S indicates the number of charged tracks at the primary vertex including the charged charm hadron and excluding any activity that can be assigned to nuclear break-up (the *black tracks*). $N_S = 2$ and $N_S = 3$ therefore would characterize the quasi-elastic production of charmed baryons of charge $+e$ and $+2e$, respectively.

4 Efficiency evaluation

Detection efficiencies were evaluated with a GEANT3 [23] based Monte Carlo simulation of the experiment. The quasi-elastic production of charmed baryons (QE) was simulated using a special event generator dedicated to that specific process (QEGEN [24]) and in which the differential cross-sections given in Ref. [5] were implemented. For the background calculation large samples of deep-inelastic neutrino interactions (DIS) were generated according to the beam spectrum by means of a Monte Carlo program (JETTA [25]) developed within CHORUS and based on LEPTO [26] and JETSET [27]. Also the contribution of D_s^+ and D_s^{*+} diffractively produced was evaluated using a program developed for this purpose [28] and included in the final background under the assumption that 50% of all D_s^+ can be assigned to diffractive processes.

To evaluate the NetScan efficiency, the emulsion data of the simulated events were merged with real NetScan data where the volume did not contain any events but only tracks which stop or pass through the volume, thus representing realistic background conditions. The performance of the automatic scanning system was also simulated using data accumulated in the NetScan procedure.

The detection efficiencies, containing both the geometrical acceptance and the reconstruction efficiency, evaluated for quasi-elastic production of charmed baryons that constitute the signal and for other DIS processes that yield Λ_c^+ , D^+ , and D_s^+ and are therefore background, are shown in Table 2 separately for the different charmed particles and for each decay topology (1-prong, 3-prong). The column labelled $DIS D_s^+$ includes also the contribution from diffractive processes. The errors quoted are those corresponding to the Monte Carlo statistics. Sources of systematic error have been considered and their effects will be included in the final result (see section 6).

		$QE (C^+)$	$QE (C^{++})$	$DIS \Lambda_c^+$	$DIS D^+$	$DIS D_s^+$
ϵ_{1p}	$N_S = 2$	0.057 ± 0.004	-	0.021 ± 0.005	0.004 ± 0.001	0.007 ± 0.003
	$N_S = 3$	-	0.074 ± 0.007	0.019 ± 0.004	0.003 ± 0.001	0.001 ± 0.001
ϵ_{3p}	$N_S = 2$	0.166 ± 0.006	-	0.044 ± 0.006	0.005 ± 0.001	0.006 ± 0.002
	$N_S = 3$	-	0.181 ± 0.009	0.022 ± 0.004	0.004 ± 0.001	0.002 ± 0.001

Table 2: Detection efficiency containing geometrical acceptance and reconstruction efficiency for decays of charmed hadrons.

5 Kinematical selection

Since quasi-elastic charmed-baryon production is characterized by low hadronic energy, a significant background rejection can be obtained on the basis of the visible energy measured in the calorimeter. To reduce the

²⁾ Among the events selected for visual inspection there are still some with a track multiplicity higher than that expected for quasi-elastic charm production because of large-angle tracks escaping the automatic scanning system.

fluctuations due to the energy loss of the primary muon in the calorimeter, only the energy measured in the first sector (EM) [29] was considered. Figure 2 shows E_{EM} , the energy measured in this sector of the calorimeter, for the candidate events. The distribution is compared with that expected for DIS production of charmed hadrons obtained with the simulation and normalized to the expected number of background events. The contribution of the diffractive production of D_s^+ and D_s^{*+} has been also included. An excess of events is visible in the energy region below 2 GeV and it is suggestive of quasi-elastic production of Λ_c^+ . Therefore, to enhance the quasi-elastic charm signal, only events with $E_{EM} \leq 2$ GeV are considered for further analysis.

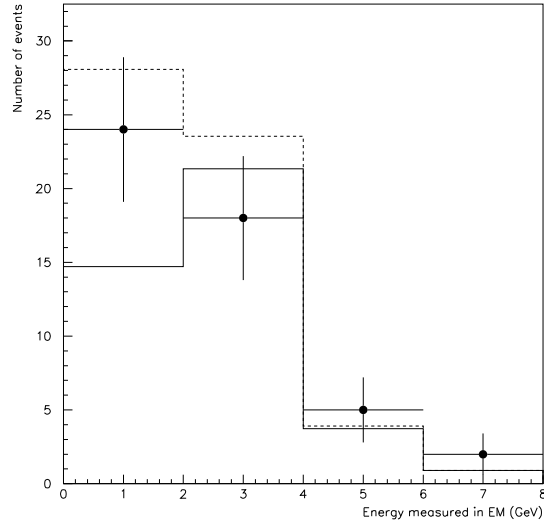


Figure 2: Energy measured in the first sector of the calorimeter (EM) for charged charm candidates. The solid line shows the energy distribution given by Monte Carlo simulation for deep inelastic charm production normalized to the expected number of background events. The dashed line shows the effect of an additional 10% contribution from quasi-elastic charm production.

A further rejection of background from non-quasi-elastic processes is obtained by studying the distribution of the angle Φ , the azimuthal angle between the primary muon and the charmed particle trajectory in the plane transverse to the incident neutrino direction.

In this plane, if the production process is quasi-elastic, the Λ_c^+ is expected to be exactly back-to-back with respect to the muon. The experimental resolution, the Fermi motion of the nucleon, and the transverse momentum carried by the (soft) pion when the Λ_c^+ is the product of decay of a Σ_c would affect Φ causing small deviations from the ideal value of 180° .

On the other hand, charmed hadrons produced through DIS processes are often accompanied by other neutral particles carrying a fraction of the hadronic energy. This fraction becomes relatively more important when the measured energy is below 2 GeV and therefore the correlation between the muon and the charmed baryon no longer exists.

In Fig. 3 the Φ distribution for events with $E_{EM} \leq 2$ GeV is compared with the Monte Carlo expectations. The predictions of the DIS Monte Carlo alone have a different shape and do not agree with the data for large values of Φ ; it is with the inclusion of a quasi-elastic contribution that a good description is obtained. On the other hand, for $\Phi \leq 150^\circ$, 10.6 events are predicted by the DIS simulation and nine are observed. In addition, it was verified that the DIS Monte Carlo describes the Φ distribution for events with $E_{EM} > 2$ GeV. The azimuthal angle Φ therefore has discriminating power and $\Phi \geq 165^\circ$ will be required to isolate the signal.

Table 3 summarizes the effects that the selections on energy and angle discussed above have on charmed baryons produced quasi-elastically and on DIS Λ_c^+ , the main component of the surviving background.

Selection	DIS Λ_c^+	QE C^+	QE C^{++}
$E_{EM} \leq 2$ GeV	0.35 ± 0.04	0.84 ± 0.01	0.83 ± 0.01
$\Phi \geq 165^\circ$	0.17 ± 0.05	0.81 ± 0.01	0.77 ± 0.01

Table 3: Efficiency of the kinematical selection on deep inelastic and quasi-elastic Λ_c^+ events

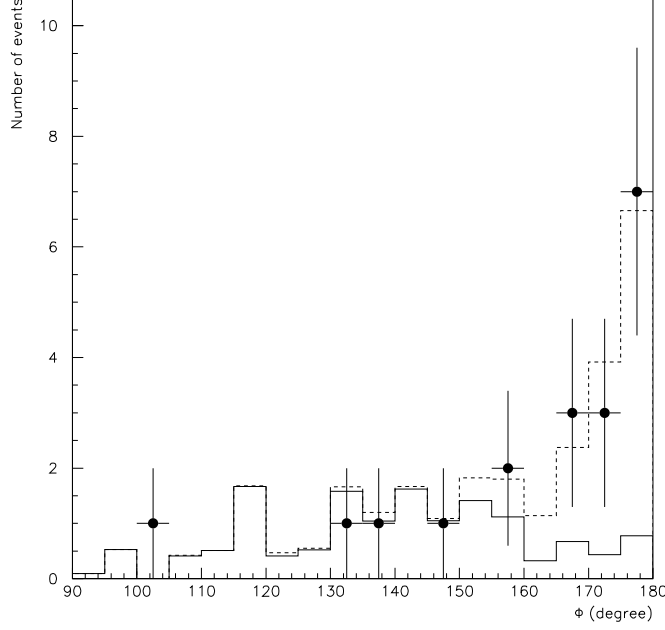


Figure 3: Azimuthal angle between the primary muon and the charmed particle trajectory in the transverse plane, for events with $E_{EM} \leq 2$ GeV. The solid and dashed lines are the expectations from deep inelastic scattering and deep inelastic scattering and quasi-elastic simulations, respectively.

6 Results and Conclusions

After the kinematical selection thirteen events survive, nine with $N_S = 2$ (2-C1, 6-C3, 1-C5) and four with $N_S = 3$ (1-C1, 3-C3). In principle, sources of background are charmed hadrons D^+ , D_s^+ , and Λ_c^+ produced in deep inelastic processes as well as D_s^+ and D_s^{*+} produced diffractively.

Using a Monte Carlo sample of events which includes at production level all these components with relative abundances fixed on the basis of the results given in Ref. [10], the number of background events with $E_{EM} \leq 2$ GeV and $\Phi \geq 165^\circ$ was computed to be 1.7 ± 0.6 . As already remarked, the selections applied reduce significantly the contribution of all channels containing a charmed meson, leaving only DIS Λ_c^+ as the dominant component.

Correcting the number of quasi-elastic candidate events with the efficiencies given in Tables 2 and 3, we obtain

$$N_{N_S=2}^{QE} = 96.1_{-27.7}^{+57.2}(\text{stat})_{-13.4}^{+10.6}(\text{syst})$$

and

$$N_{N_S=3}^{QE} = 37.7_{-20.4}^{+42.8}(\text{stat})_{-5.3}^{+4.1}(\text{syst})$$

for the quasi-elastic processes (1)–(2) and (3), respectively. The systematic error includes the effect of Monte Carlo statistics used for the efficiency evaluation, instrumental effects, error on background evaluation, and differences in the Q^2 dependence in the simulation of the quasi-elastic charmed-baryon production.

The ratio of the location efficiency of the different charm-producing processes relative to ν_μ CC interactions has been evaluated [10] using real data and the Monte Carlo muon momentum spectrum. For quasi-elastic charm events this ratio is 1.24 ± 0.01 .

As already stated, this analysis is restricted to events where the measured momentum of the muon lies below 30 GeV. However, Monte Carlo studies show that this does not introduce a bias since its effect on the quasi-elastic charm production rate relative to ν_μ CC interactions is only a fraction of a percent, due to cancellations in the ratio.

Therefore, normalizing to the number of CC events in the sample, a value of

$$\sigma(QE)/\sigma(CC) = (0.23_{-0.06}^{+0.12}(\text{stat})_{-0.03}^{+0.02}(\text{syst})) \times 10^{-2}$$

is obtained for the ratio of the cross-sections for quasi-elastic production of charmed baryons and νN CC interactions.

In the same manner it is possible to obtain the cross-section ratios

$$\sigma(C^+)/\sigma(CC) = (0.17_{-0.05}^{+0.10}(\text{stat}) \pm 0.02(\text{syst})) \times 10^{-2}$$

and

$$\sigma(C^{++})/\sigma(CC) = (0.07_{-0.04}^{+0.07}(stat) \pm 0.01(syst)) \times 10^{-2}$$

for the production of charmed baryons of charge $+e$ and $+2e$, respectively.

Isospin properties imply [2]–[8] that

$$\sigma(\nu p \rightarrow \mu^- \Sigma_c^{++}) + \sigma(\nu p \rightarrow \mu^- \Sigma_c^{*++}) = 2(\sigma(\nu n \rightarrow \mu^- \Sigma_c^+) + \sigma(\nu n \rightarrow \mu^- \Sigma_c^{*+}))$$

Since nuclear emulsions are approximately isoscalar, the above relation can be used with the measured values of the cross-sections to conclude that in quasi-elastic νN scattering Λ_c and Σ_c baryons are produced at an almost equal rate.

Among the various models, the measured value of the cross-section seems to prefer those that introduce *suppression* factors to simple quark models, like [3] and [8].

Combining the result obtained in this paper with that given in Ref. [10] – where the total production of Λ_c was measured – we can conclude that 0.15 ± 0.09 of all Λ_c baryons are produced through quasi-elastic processes.

In quasi-elastic events, conservation of transverse momentum at the primary vertex allows the momentum of the charmed baryon to be estimated and therefore to reconstruct completely the event kinematics. This reconstruction however is only approximate since Fermi motion and the momentum of the pion that might come from Σ_c decays are neglected.

Figure 4 shows the Q^2 distribution obtained from the thirteen quasi-elastic charm candidate events. The observed average value of this quantity is $\langle Q^2 \rangle_{obs} = (2.0 \pm 0.6) \text{ GeV}^2$.

The histogram is the result of a Monte Carlo simulation with the model of Ref. [5]. Despite large discrepancies in the total cross-section predictions, the various models [3]–[8] give similar Q^2 behaviour and the present data do not have sufficient resolution to discriminate them.

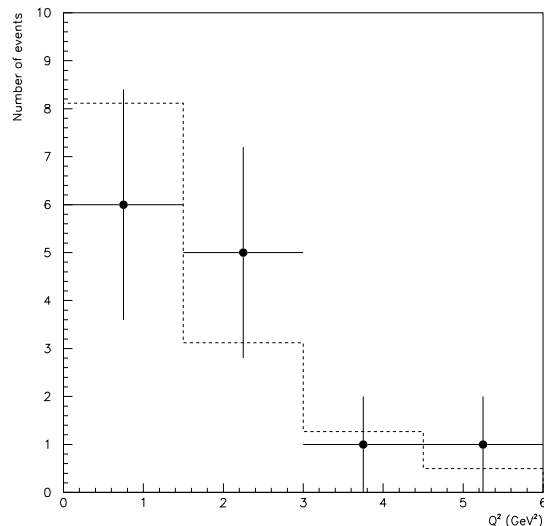


Figure 4: Q^2 distribution for the observed quasi-elastic charm candidates. The histogram is the result of a Monte Carlo simulation with the model of Ref. [5].

The sample analysed for this paper is only a quarter of what is available in CHORUS and therefore the analysis of the complete sample is expected to improve the statistical error significantly.

Acknowledgments

We gratefully acknowledge the help and support of the neutrino beam staff and of the numerous technical collaborators who contributed to the detector construction, operation, emulsion pouring, development and scanning. The experiment has been made possible by grants from: the Institut Interuniversitaire des Sciences Nucléaires and the Interuniversitair Instituut voor Kernwetenschappen (Belgium), the Israel Science Foundation (grant 328/94) and the Technion Vice President Fund for the Promotion of Research (Israel), CERN (Geneva, Switzerland), the German Bundesministerium für Bildung und Forschung (Germany), the Institute of Theoretical and Experimental Physics (Moscow, Russia), the Istituto Nazionale di Fisica Nucleare (Italy), the Promotion and Mutual Aid Corporation for Private Schools of Japan and Japan Society for the Promotion of Science (Japan), the

Korea Research Foundation Grant (KRF-2001-005-D00006) (Republic of Korea), the Foundation for Fundamental Research on Matter FOM and the National Scientific Research Organization NWO (The Netherlands) and the Scientific and Technical Research Council of Turkey (Turkey). We gratefully acknowledge their support.

References

- [1] N. Armenise et al., Phys. Lett. **B86** (1979) 15.
- [2] J. Finjord and F. Ravndal, Phys. Lett. **B58** (1975) 61.
- [3] A. Amer, M.B. Gavela, A. Le Yaouanc and L. Oliver, Phys. Lett. B **B81** (1979) 48.
- [4] S.G. Kovalenko, Sov. J. Nucl. Phys. **52** (1990) 934.
- [5] R.E. Shroch and B.W. Lee, Phys. Rev. **D13** (1976) 2539.
- [6] C. Avilez, T. Kobayashi and J.C. Korner, Phys. Lett. **B66** (1977) 149.
- [7] C. Avilez, T. Kobayashi and J.C. Korner, Phys. Rev. **D17** (1978) 709.
- [8] C. Avilez and T. Kobayashi, Phys. Rev. **D19** (1979) 3448.
- [9] P. Migliozi, G. D'Ambrosio, G. Miele and P. Santorelli, Phys. Lett. **B462** (1999) 217.
- [10] Kayis-Topaksu et al., CHORUS Collaboration, Phys. Lett. **B555** (2003) 156.
- [11] H. Grassler et al., WA21 Collaboration, Phys. Lett. **B99** (1981) 159.
- [12] N. Armenise et al., Phys. Lett. **B104** (1981) 409.
- [13] P.C. Bosetti et al., WA21 Collaboration, Phys. Lett. **B109** (1982) 234.
- [14] D. Son et al., Phys. Rev. **D28** (1983) 2129.
- [15] G.T. Jones et al., WA21 Collaboration, Z.Phys. **C36** (1987) 593.
- [16] V.V. Ammosov et al., JETP Lett. **58** (1993) 247.
- [17] Particle Data Group, K. Hagiwara et al., Phys. Rev. **D66** (2002) 010001.
- [18] N. Ushida et al., E531 Collaboration, Phys. Lett. **B206** (1988) 375.
- [19] E. Eskut et al., CHORUS Collaboration, Nucl. Instrum. Methods **A401** (1997) 7.
- [20] T. Nakano, Ph.D thesis, Nagoya University, Japan, 1997.
- [21] T.Nakano, Proceedings of International Europhysics Conference on HEP 2001.
- [22] K. Kodama, et al., Nuclear Instrum. Methods **A493**, (2002) 45.
- [23] GEANT 3.21, CERN Program Library Long Writeup W5013.
- [24] F. Di Capua, Ph.D thesis, Università di Napoli, Italy (2003).
- [25] P. Zucchelli, Ph.D thesis, Università di Ferrara, Italy (1995).
- [26] G. Ingelman, Preprint TSL/ISV 92-0065, Uppsala University, Sweden (1992)
- [27] T. Sjostrand, Comp. Phys. Comm. **82**, (1994) 74.
- [28] O. Melzer, Diploma Thesis, Westfälische Wilhelms-Universität, Münster, 1997
O. Melzer and J. Goldberg, CHORUS Internal Note 2000008, unpublished.
- [29] E. Di Capua et al., Nucl. Instrum. Methods **A378** (1996) 221.